Friday Harbor
SEA: Spring Bloom and Submarine Canyons

S.E. Allen

August 2, 2019

Chapter 1

Spring Phytoplankton Bloom

1.1 Learning Goals

By the end of this lecture and appropriate revision/study, students will be able to:

- define the spring phytoplankton bloom
- describe the Sverdrup Critical Depth Hypothesis for the Spring Phytoplankton Bloom
- explain several physical processes that impact spring bloom timing in coast/estuarine waters beyond those included in the Sverdrup hypothesis
- define mixed and mixing layer
- define and use the bulk Richardson number

1.2 Class Time Structure

- **Mini-Lecture** Spring Phytoplankton Bloom in the Strait of Georgia
- **Worksheet** Sverdrup's Critical Depth Hypothesis
- **Mini-Lecture** SOG and how it works
- **Discussion** Estuarine/coastal physics and its impacts on the timing of the spring bloom
- **Summary and Implications**

1.3 Spring Phytoplankton Bloom in the Strait of Georgia

- phytoplankton
- satellite observation
- ferry observations
- interannual variability in the spring bloom
- what phytoplankton need to grow
- what initiates the spring bloom?
- what ends the spring bloom?

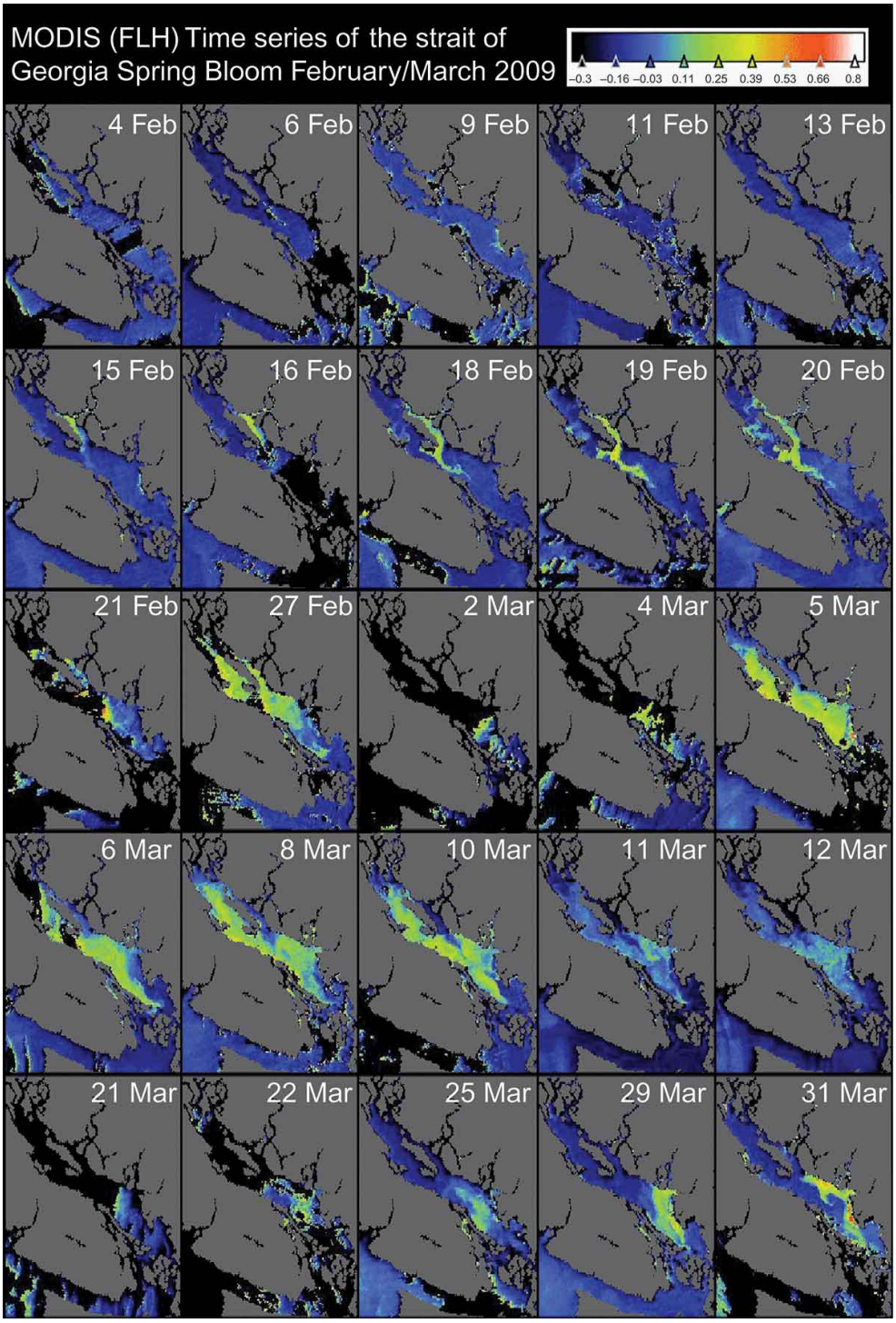

Figure 1.1: Time series of MODIS FLH images showing the start of the spring bloom in the Strait of Georgia in 2009. Clouds are masked to black and land to grey. Only relatively cloud-free scenes are shown. The legend shows values of FLH in radiance units (mW m^{-2} nm^{-1} sr^{-1}). Figure 4 from Gower and King (2012).

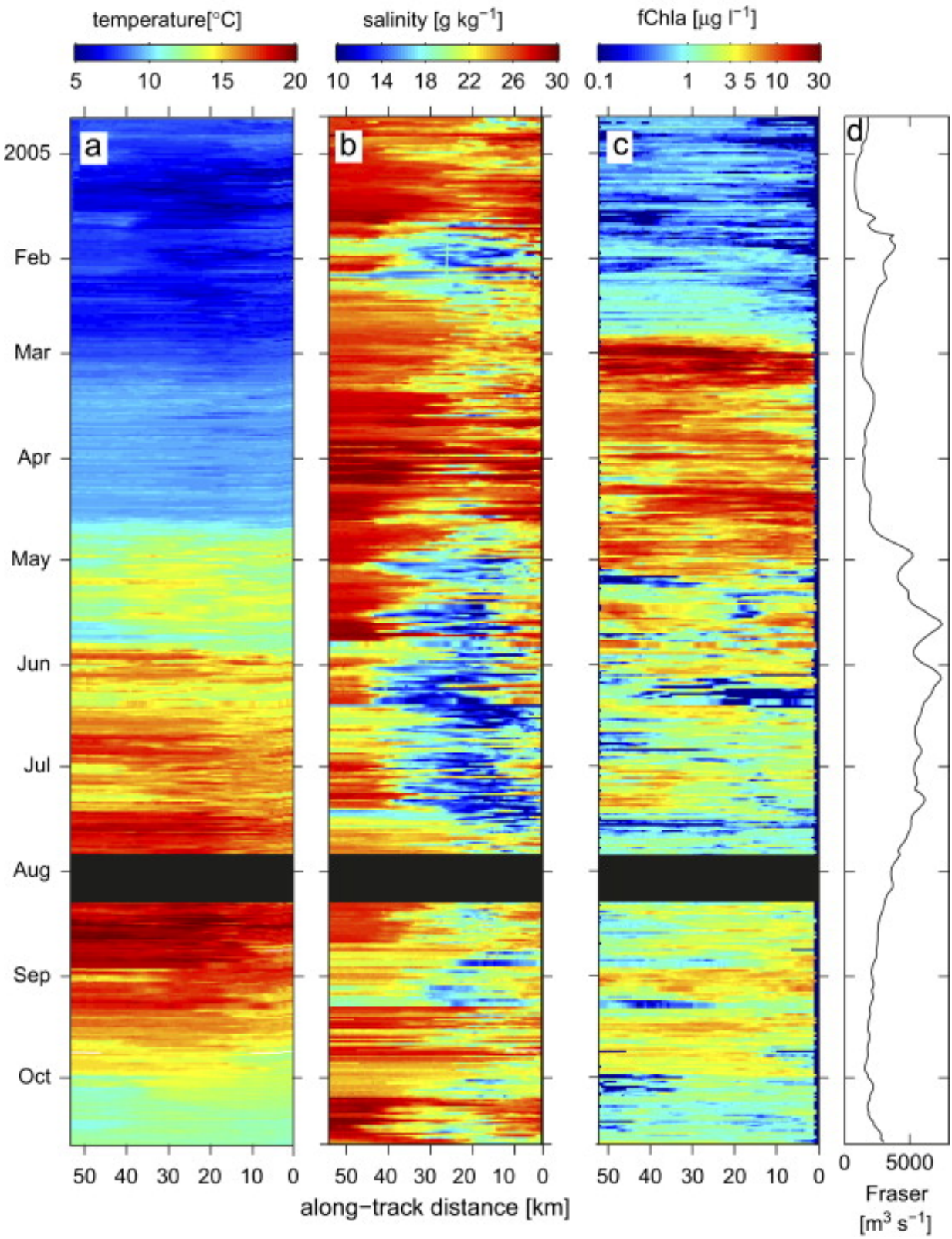

Figure 1.2: Hovmöller diagram for the 2005 ferry-measured (a) temperature, (b) salinity, and (c) raw in situ chlorophyll-a (fChla). The black areas represent missing data. The Fraser River discharge, as measured at Hope by Environment Canada, is shown in panel d. Figure 6 from Halverson and Pawlowicz (2013).

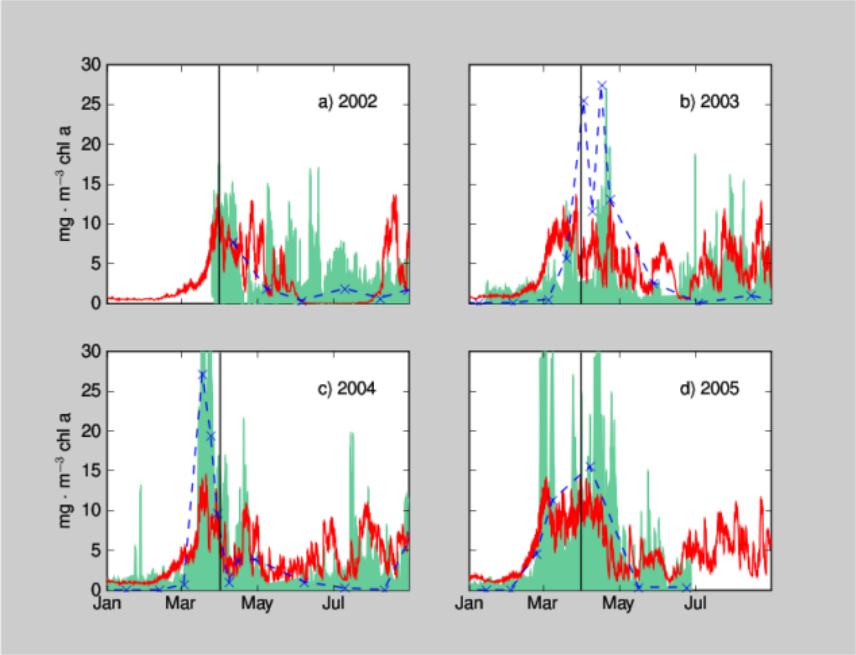

Figure 1.3: Modeled surface phytoplankton (solid red line), ferry fluorescence (green shading), and bottle-sampled (>20 m) chlorophyll (blue xs connected by broken line) for each year: (a) 2002; (b) 2003; (c) 2004; and (d) 2005. Ferry fluorescence absolute scale is poorly known and possibly changed between years. Vertical line marks 1 April each year. Figure 8 from Collins et al. (2009)

Worksheet: Sverdrup's Critical Depth Hypothesis*

Phytoplankton need light to grow. If you work in a lab and calculate oxygen evolution (a measure of growth) versus light you get a curve something like that shown in Figure 1.4. Note that growth is zero at some finite light intensity, where cellular respiration is balanced by cellular photosynthesis. This is the compensation light intensity, I_c, typically 10 μ E m^{-2} s^{-1} or approximately 5 W m^{-2}*.

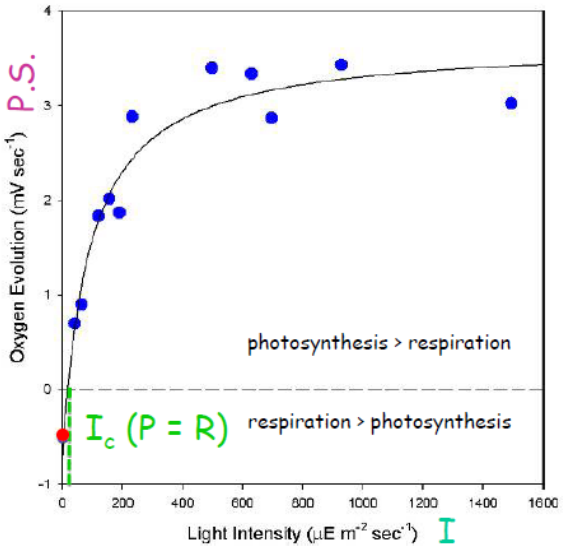

Figure 1.4: Photosynthetic growth measure by oxygen evolution. Figure courtesy Maite Maldonado.

1. If we assume light decreases with depth, exponentially at a constant rate $\kappa = (5\mathrm{m})^{-1}$, and that the surface light intensity, I_o is 100 W m^{-2} calculate the compensation depth, H_c. The depth at which a phytoplankton would have zero growth.

*Based on a lecture written by Prof. Maite Maldonado.

*Considering that only the 400-700 nm range of light is available to the phytoplankton

2. Consider now that the phytoplankton does not stay at a constant depth because it is in a surface mixing layer. If the mixing layer has a depth $H_m = H_c$, and the phytoplankton sample all depths above that evenly, what is the average light the phytoplankton receives? Does the phytoplankton grow or die?

3. How deep can the mixing layer be and the phytoplankton grow? This depth is Sverdrup's critical depth and his hypothesis is that the spring bloom will occur if/when the mixed layer depth is shallower than the critical depth. Is the critical depth shallower or deeper than the compensation depth? Why?

1.4 SOG Model

- NP model
- KPP mixing model
- Mixing depth determination
- Forcing

$$Ri_b(d) = \frac{(B_r - B(d))d}{\|V_r - V(d)\|^2 + V_t^2(d)} \tag{1.1}$$

where Ri_b is the bulk Richardson number, d depth, B_r near surface buoyancy flux, $B(d)$ buoyancy at depth d, V_r near surface velocity, $V(d)$ velocity at depth d, V_t turbulent velocity shear. Equation (21) from Large et al. (1994).

1.5 Estuarine/Coastal Process

- What physical processes are neglected by the Sverdrup CDM?
- Which of them are 1-D, 2-D and 3-D processes?
- Would they tend to accelerate (earlier) spring bloom? or delay the spring bloom?
- Can they be parametrized in a 1-D model?

1.6 Summary and Implications

- The spring bloom in the Strait of Georgia according to SOG
- Physical dependencies
- Known errors
- Implications to higher trophic levels

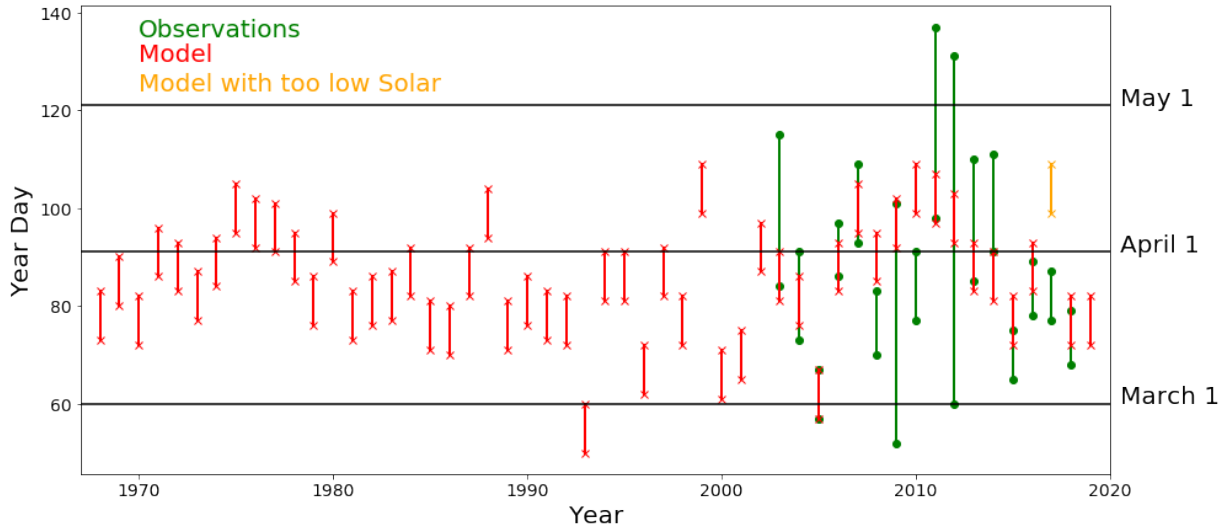

Figure 1.5: Time series of the timing of the peak of the Spring Phytoplankton Bloom. Green- observations from the ferry systems. Green star- approximate value for 2018. Red SOG model. Orange SOG model with too little solar radiation. Figure 3 of Allen et al. (2018).

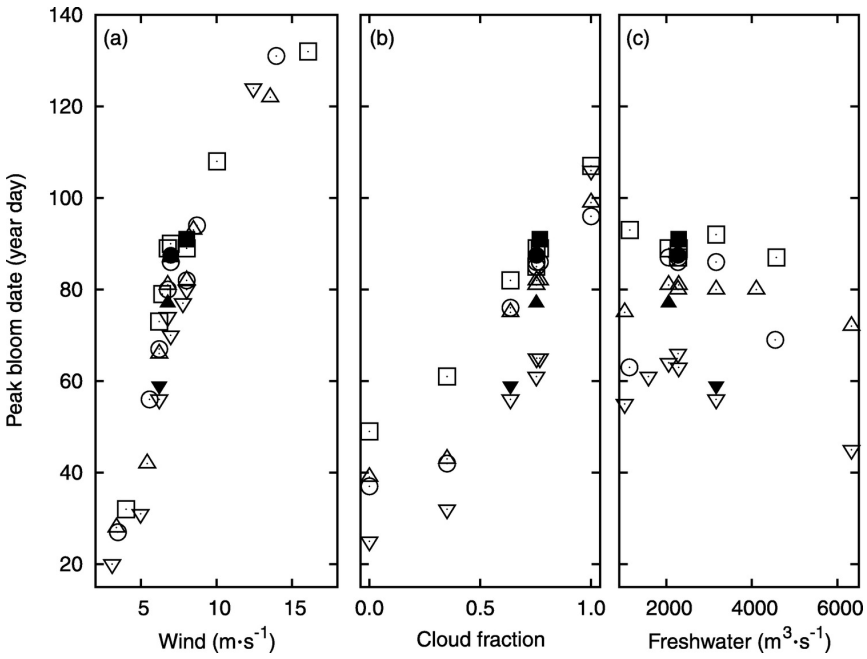

Figure 1.6: Results of model testing gave different bloom arrival dates for different wind (cubed root of the average December to February wind speed cubed), cloud patterns (average cloud fraction from December to January), and freshwater flow (average effective total freshwater from December to January). Solid symbols represent actual peak bloom. As wind magnitude increases, the arrival date of the bloom is later; this relationship is strong. Cloud fraction plays a secondary role in the timing of the bloom. There is no clear relationship between date of bloom peak and river flow. Figure 11 from Collins et al. (2009).

Bibliography

Allen, S. E., Olson, E., Latornell, D., Pawlowicz, R., Do, V., Stankov, K., and Esendulova, S. (2018). Spring phytoplankton bloom timing, interannual summer productivity in the Strait of Georgia. In Chandler, P., King, S., and Boldt, J., editors, *State of the physical, biological and selected fishery resources of Pacific Canadian marine ecosystems in 2017*, volume 3266 of *Can. Tech. Rep. Fish. Aquat. Sci.*, pages 164–169.

Allen, S. E. and Wolfe, M. A. (2013). Hindcast of the timing of the spring phytoplankton bloom in the Strait of Georgia, 1968-2010. *Progr. Ocean*, 115:6–13.

Collins, A. K., Allen, S. E., and Pawlowicz, R. (2009). The role of wind in determining the timing of the spring bloom in the Strait of Georgia. *Can. J. Fish. Aquat. Sci.*, 66:1597–1616.

Gower, J. and King, S. (2012). Use of satellite images of chlorophyll fluorescence to monitor the spring bloom in coastal waters. *International journal of remote sensing*, 33(23):7469–7481.

Halverson, M. J. and Pawlowicz, R. (2013). High-resolution observations of chlorophyll-a biomass from an instrumented ferry: Influence of the fraser river plume from 2003 to 2006. *Continental Shelf Research*, 59:52–64.

Large, W. G., McWilliams, J. C., and Doney, S. C. (1994). Oceanic vertical mixing: A review and a model with a nonlocal boundary layer parameterization. *Rev. Geophys.*, 32(4):363–403.

Sverdrup, H. U. (1953). On conditions for the vernal blooming of phytoplankton. *J. Conseil. Exp. Mer.*, 18:287–295.

Wolfe, A. M., Allen, S. E., Hodal, M., Pawlowicz, R., Hunt, B. P., and Tommasi, D. (2015). Impact of advection loss due to wind and estuarine circulation on the timing of the spring phytoplankton bloom in a fjord. *ICES Journal of Marine Science*, 73(6):1589–1609.

Chapter 2

Submarine Canyons

2.1 Learning Goals

By the end of this lecture and appropriate revision/study, students will be able to:

- explain and show mathematically why homogenous geostrophic flow follows isobaths
- describe why even stratified flow usually follows isobaths
- list three processes that can "break the constraints" and allow flow across isobaths
- explain arrested bottom boundary layers
- describe dynamically why alongshore flow causes upwelling/downwelling through canyons
- explain how enhanced mixing in canyons changes the amount of "tracer" upwelled onto the shelf

2.2 Class Time Structure

- **Mini-Lecture** Constraints on Flow across Bathymetry
- **Worksheet** Arrested Bottom Boundary Layers
- **Mini-Lecture** Flow through Canyons
- **All Together** Scaling the Depth of Upwelling
- **Mini-Lecture** Impact of Mixing

2.3 Constraints of Flow across Bathymetry

- homogeneous constraint Allen (2004), Section 1
- stratified constraints Brink (1998)
- breaking the constraints

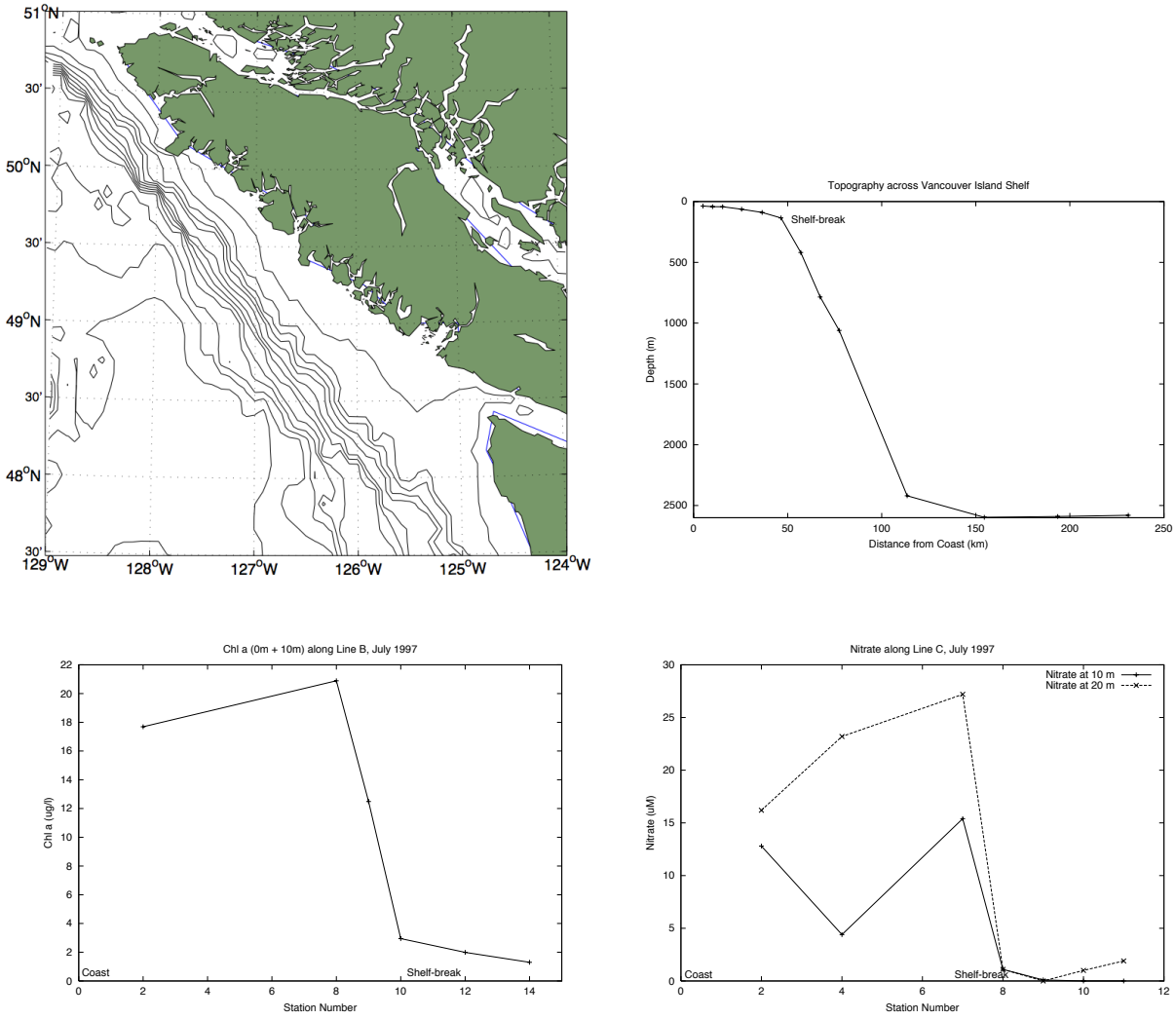

Figure 2.1: Bathymetry of the West Coast of Vancouver Island as a map with contours 200 m apart (upper left) and as a depth cross-section (upper right). 10-m averaged phytoplankton Chlorophyll across the same section (lower left) and 10 m and 20 m nitrate across the same section (lower right). Figures 3, 1, 4 and 5 from Allen (2004)

Following Brink (1998), the steady, weak (aka linear), inviscid, Boussinesq flow equations are:

$$fv = \frac{1}{\rho_o}\frac{\partial p}{\partial x} \tag{2.1}$$

$$-fu = \frac{1}{\rho_o}\frac{\partial p}{\partial y} \tag{2.2}$$

$$\frac{\partial p}{\partial z} = -\rho g \tag{2.3}$$

$$0 = \frac{\partial u}{\partial x} + \frac{\partial v}{\partial y} + \frac{\partial w}{\partial z} \tag{2.4}$$

$$0 = u\frac{\partial \rho}{\partial x} + v\frac{\partial \rho}{\partial y} + w\frac{\partial \rho}{\partial z} \tag{2.5}$$

Equations (2.1) and (2.2), with f constant imply $\partial w/\partial z = 0$, as before. At the top, nearly flat, $w = 0$ at the bottom the flow must be zero in or out of the bottom so

$$u\frac{\partial h}{\partial x} + v\frac{\partial h}{\partial y} + w = 0 \tag{2.6}$$

However, if w is zero then the flow at the bottom must be parallel to the isobaths.
Note that (2.1), (2.2) and (2.3) combine to give the thermal wind equations:

$$f\frac{\partial v}{\partial z} = \frac{-1}{\rho}\frac{\partial \rho}{\partial x} \tag{2.7}$$

$$f\frac{\partial u}{\partial z} = \frac{1}{\rho}\frac{\partial \rho}{\partial y} \tag{2.8}$$

Now with $w = 0$ (2.5) becomes $u\partial\rho/\partial x + v\partial\rho/\partial y = 0$. Substituting the thermal wind equations above we get

$$-u\frac{\partial v}{\partial z} + v\frac{\partial u}{\partial z} = 0 \tag{2.9}$$

or

$$(u, v) \times \frac{\partial}{\partial z}(u, v) = 0 \tag{2.10}$$

So the vertical shear is parallel to flow unless the flow goes to zero. So from the bottom, up until the flow goes through zero, the flow must be parallel the to bathymetry.
The full x-momentum equation is:

$$\frac{\partial u}{\partial t} + u\frac{\partial u}{\partial x} + v\frac{\partial u}{\partial y} - fv = \frac{-1}{\rho_o}\frac{\partial p}{\partial x} + \frac{\partial}{\partial z}\left(A\frac{\partial u}{\partial z}\right) \tag{2.11}$$

2.4 Arrested Bottom Boundary Layer: Worksheet

Worksheet: Arrested Bottom Boundary Layers

If we consider flow over a flat bottom boundary in a system where rotation matters, we get an Ekman boundary layer. The depth of the Ekman layer is $\delta = (2\nu/f)^{1/2}$ where ν is the effective vertical eddy viscosity. There is a mass flux in the boundary layer, perpendicular to the flow of δu_θ where u_θ is the azimuthal velocity above the boundary layer.
A video of this process in a rotating tank is available here: `https://www.youtube.com/watch?v=LSm-9x3G6C8`
This bottom boundary layer is a steady solution to the equations for an infinite domain with the a uniform current.
Consider now flow over a slope. If the fluid is homogeneous, the Ekman layer is little changed (Pedlosky, 1979). The Ekman layer thickness is $\delta_s = (2\nu/f\cos\alpha)^{1/2}$ where α is the slope. The flux along the slope becomes $\delta_s u_\theta$ which is slightly bigger than for the flat bottom case. Again, given an infinite domain (hard with a slope I agree) and a uniform current this solution is steady.
Now consider stratified flow over a slope. Consider along the isobaths with the shallow water to the left.

1. What direction is the initial Ekman flow in?

2. What does that do to the isopycnals?

3. Considering that the overlying geostrophic flow is v_g (a negative value), what is the pressure gradient? We will call this the background pressure gradient.

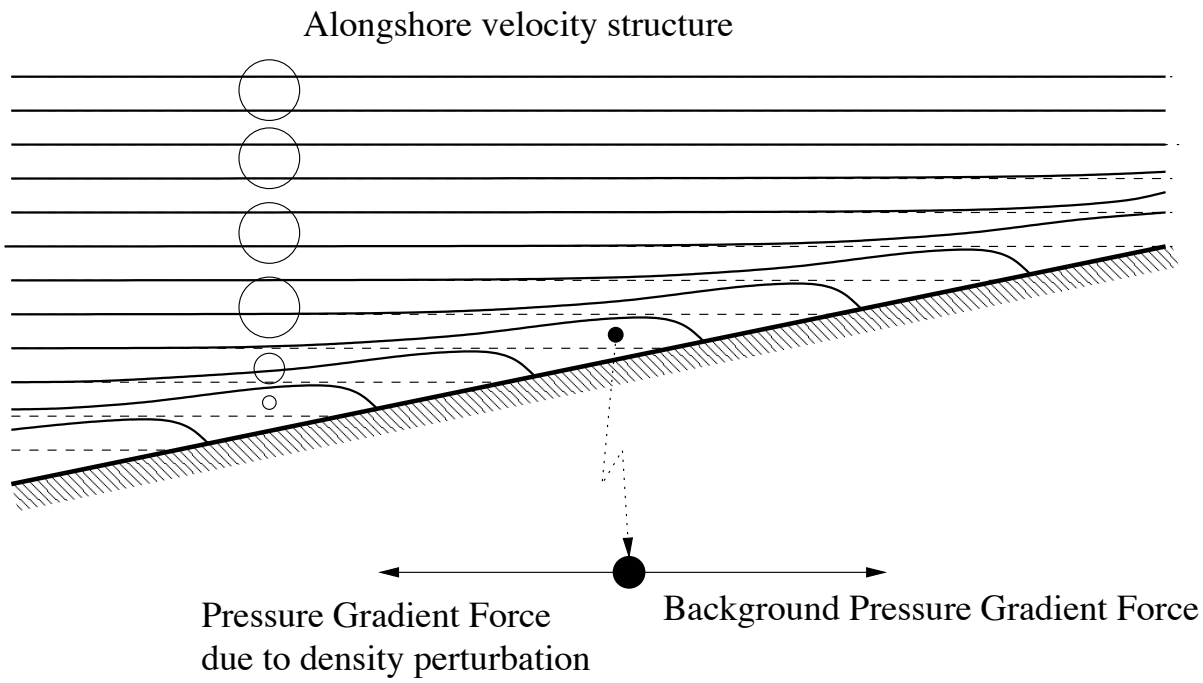

Figure 2.2: From Allen (2004), sketch of isopycnals during upwelling favourable alongslope flow.

4. Using Figure 2.2 as a guide, what is the baroclinic pressure gradient caused by the tilting isopycnals, given a background stratification of:

$$N^2 = \frac{-g}{\rho_o}\frac{\partial \rho}{\partial z}$$

and a run-up length of the isopycnals of X.

5. Balancing the background pressure gradient force and the baroclinic pressure gradient, what is the run-up X?

6. Given a geostrophic flow of 0.2m s^{-1}, a Coriolis parameter of 1×10^{-4} s^{-1} a stratification of $N = 5 \times 10^{-3}$s^{-1} and a strong, canyon like slope of 0.1, what is the run-up?

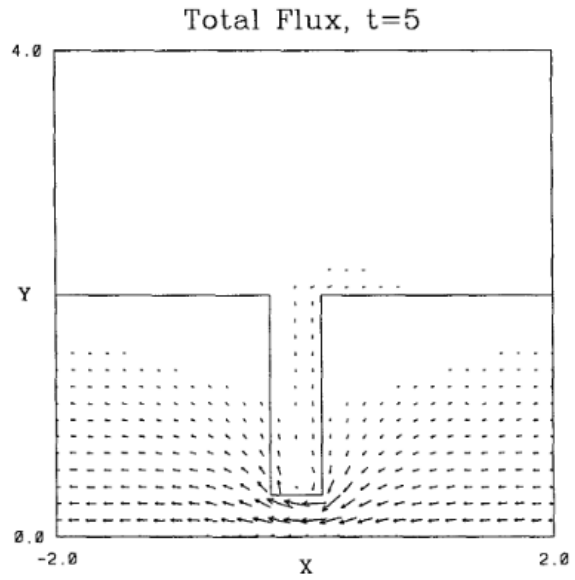

Figure 2.3: Total flux over a canyon using linear dynamics. Showing the symmetry of the bent shelf-break current around the canyon and the upwelling through the canyon. Upwelled water is symmetric. Figure 8 from (Allen, 1996).

2.5 Flow through Canyons

- Freeland and Denman (1982) basic understanding
- time dependent upwelling/downwelling
- downwelling
- advection-driven upwelling

2.6 Scaling the Depth of Upwelling

- What quantities should matter?
- Should increase each of them, increase or decrease the depth of upwelling?
- What dimensions do they have?
- How many non-dimensional groups can we make?
- What is our best estimate of the scale for the depth of upwelling?

2.7 Impact of Mixing

- Canyons transport material onto the shelf
- Material can get to the surface layer through instabilities
- Canyons are regions of enhanced internal waves
- Enhanced mixing can increase flux onto the shelf

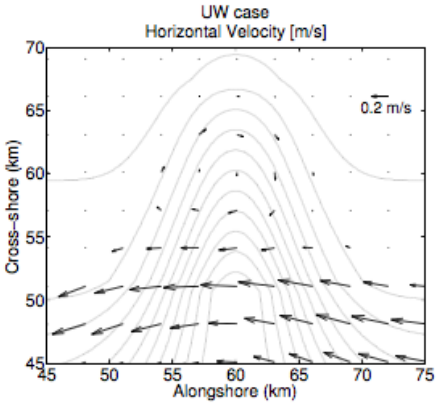

(a) Anticyclonic circulation

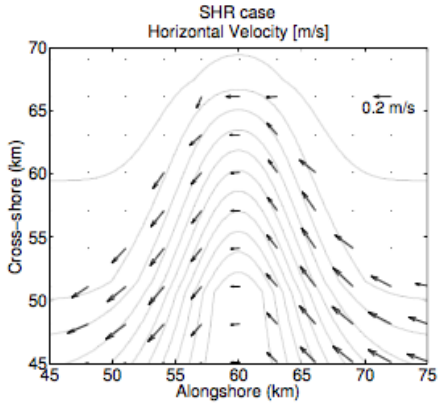

(b) Cyclonic circulation

Figure 2.4: Flow patterns just above shelf-break depth for downwelling canyons. Two different patterns but note how symmetric they are. These are numerical solutions with full nonlinear terms. Figure 6 from (Spurgin and Allen, 2014).

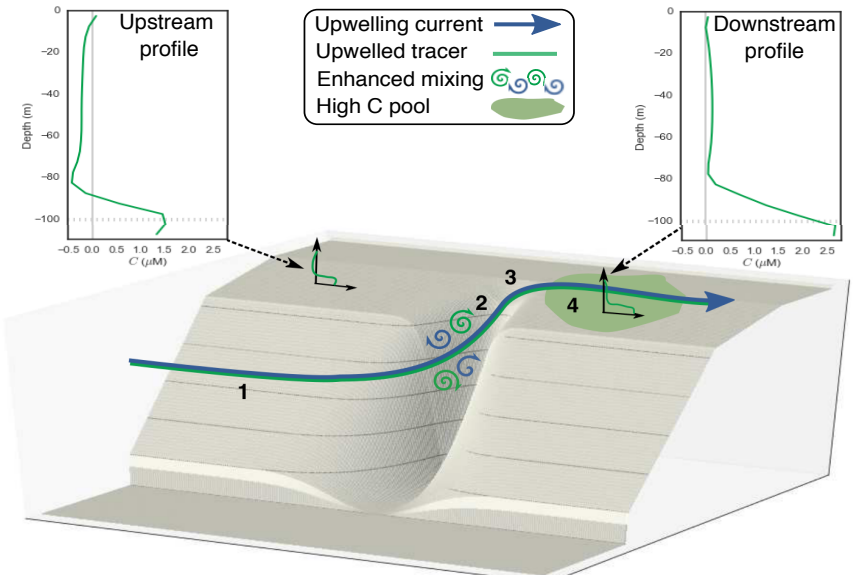

Figure 2.5: Schematic of upwelling flow (driven by advection) over a submarine canyon. Figure 11 from Ramos-Musalem and Allen (2019).

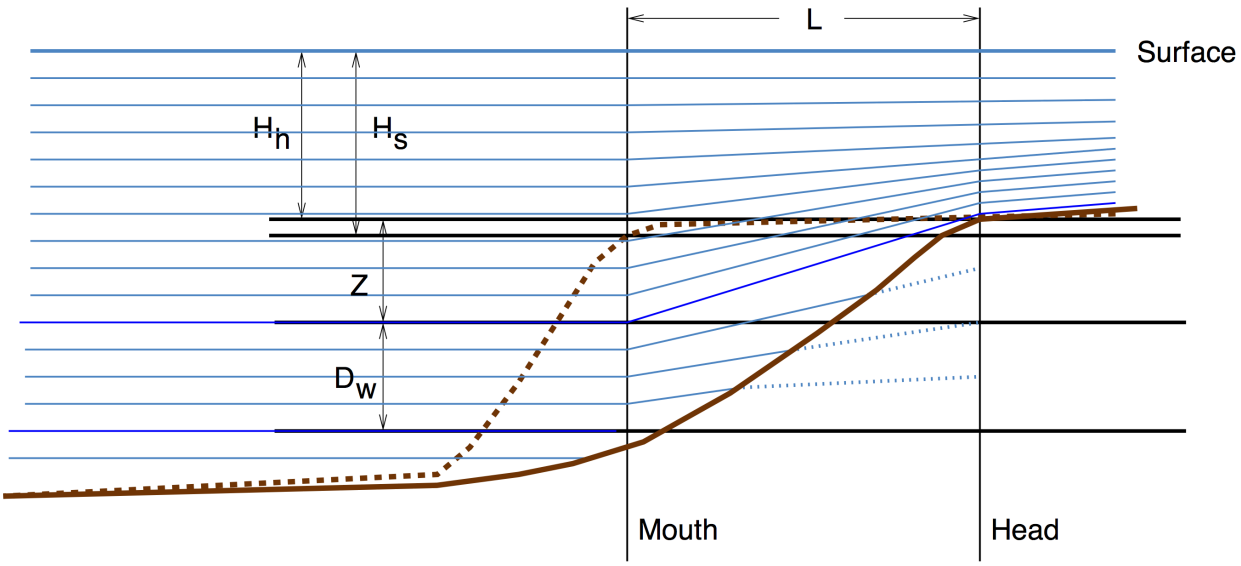

Figure 2.6: Sketch to illustrate the baroclinic pressure gradient due to isopycnals (fine lines) tilting towards the head of the canyon. The sketch shows a cross-section through the centreline of the canyon. The bottom-topography away from the canyon is given by the bold dashed line. The height Z is determined by balancing the pressure gradient at rim-depth and the change in baroclinic pressure gradient due to the tilted isopycnals. The depth $H_h + Z$ is the deepest water upwelled onto the shelf. Figure 3 from Allen and Hickey (2010)

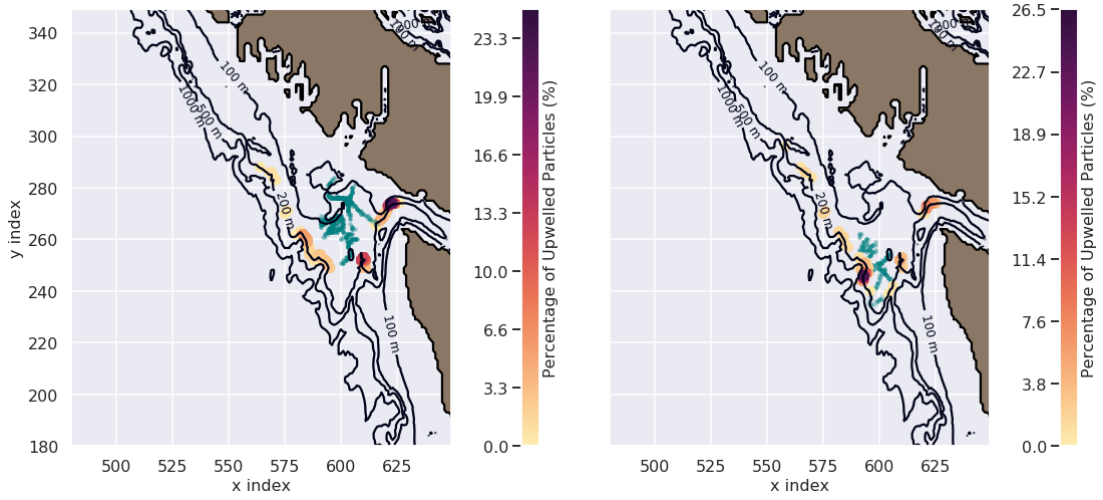

Figure 2.7: Where the particles on the shelf (blue) cross the shelf-break (yellow-purple scale). Sahu et al., in prep

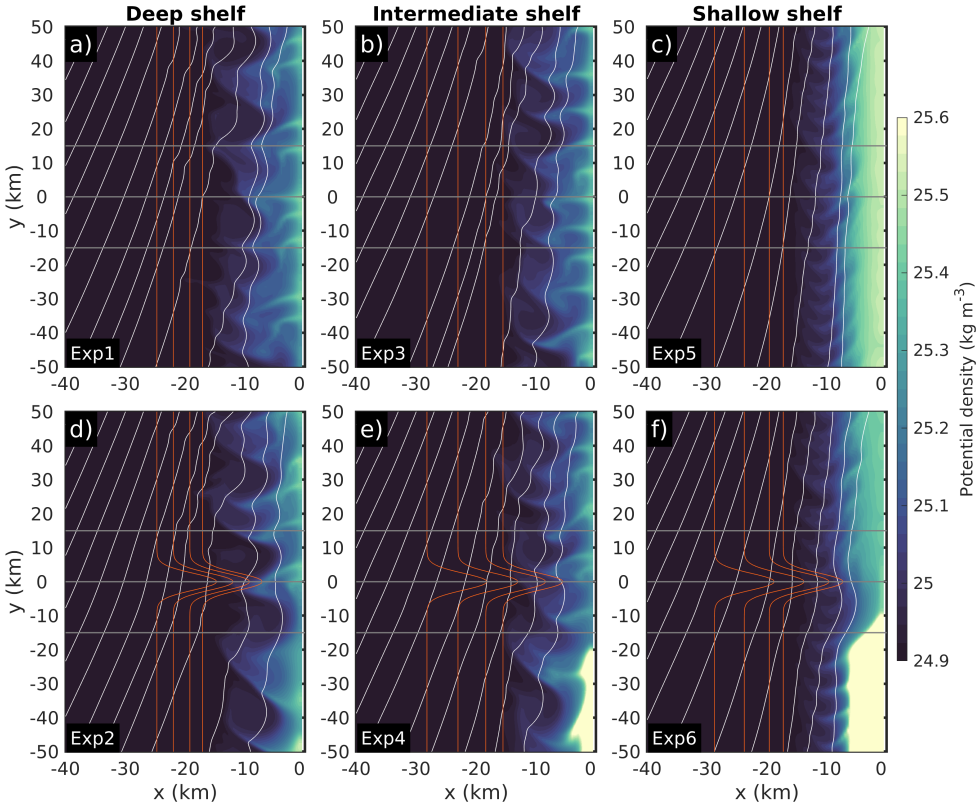

Figure 2.8: Surface Density for Baroclinic Instability Flat Shelf (top row) with a Canyon (lower row). Figure 3 from Salidias and Allen, in revision.

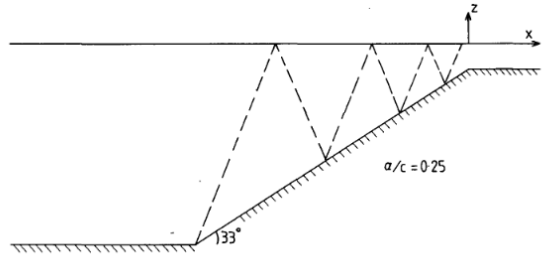

FIG. 13. Typical rays for the internal waves for $\alpha/c = 0.25$.

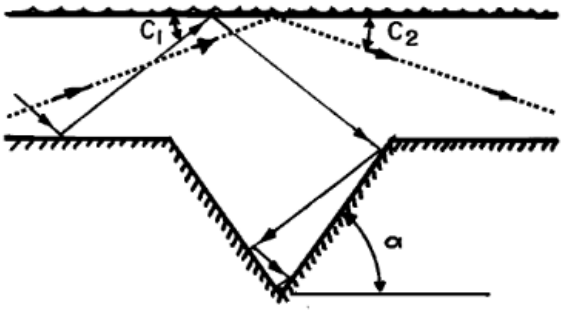

Fig. 3. Illustration of proposed mechanism for internal wave trapping. Waves whose energy propagation ray slope, C, is smaller than α may become trapped. All waves in the EB and below satisfy this criterion. However, waves with wavelengths sufficiently long relative to the width of the canyon will largely remain free from trapping.

Figure 2.9: Internal wave rays in canyons. Internal waves from outside tend to be trapped within canyons whether they come in the mouth or down from above. Figure 13 from Baines (1983) and Figure 3 from Gordon and Marshall (1976)

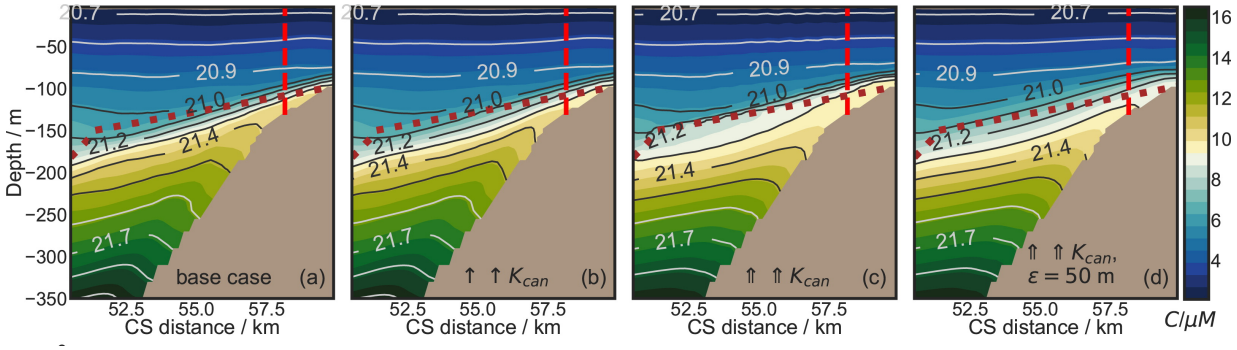

Figure 2.10: Impact of increased diffusivity on canyon upwelling. Figure 3 from Ramos-Musalem and Allen (2019).

Bibliography

Allen, S. E. (1996). Topographically generated, subinertial flows within a finite length canyon. *J. Phys. Oceanogr.*, 26:1608–1632.

Allen, S. E. (2004). Restrictions on deep flow across the shelf-break. *Surveys in Geophysics*, 25:221–247.

Allen, S. E. and Hickey, B. M. (2010). Dynamics of advection-driven upwelling over a submarine canyon. *J. Geophys. Res.*, 115. Art. No. C08018, doi:10.1029/2009JC005731.

Baines, P. G. (1983). Tidal motion in submarine canyonsa laboratory experiment. *Journal of Physical Oceanography*, 13(2):310–328.

Brink, K. H. (1998). Deep-sea forcing and exchange processes. In Brink, K. H. and Robinson, A. R., editors, *The global coastal ocean, processes and methods*, number 10 in The Sea, pages 151–167. John Wiley and Sons, New York, New York.

Freeland, H. J. and Denman, K. L. (1982). A topographically controlled upwelling center off southern Vancouver Island. *J. Mar. Res.*, 40:1069–1093.

Gordon, R. and Marshall, N. (1976). Submarine canyons: Internal wave traps? *Geophysical Research Letters*, 3(10):622–624.

Pedlosky, J. (1979). *Geophysical Fluid Dynamics*. Springer-Verlag, New York.

Ramos-Musalem, K. and Allen, S. E. (2019). The impact of locally enhanced vertical diffusivity on the cross-shelf transport of tracers induced by a submarine canyon. *Journal of Physical Oceanography*, 49(2):561–584.

Spurgin, J. M. and Allen, S. E. (2014). Flow dynamics around downwelling submarine canyons. *Ocean Sci.*, 10:799–819.